Engineering Fracture Mechanics 77 (2010) 2263–2276

Contents lists available at ScienceDirect

Engineering Fracture Mechanics

journal homepage: www.elsevier.com/locate/engfracmech

Improved sequentially linear solution procedure

Jan Eliáš *, Petr Frantík, Miroslav Vořechovský

Institute of Structural Mechanics, Faculty of Civil Engineering, Brno University of Technology, Veveří 95, 602 00 Brno, Czech Republic

ARTICLE INFO

Article history:
Received 21 May 2009
Received in revised form 13 May 2010
Accepted 16 May 2010

Keywords:
Sequentially linear procedure
Elasto-brittle elements
Non-proportional load-path
Stress redistribution

ABSTRACT

The article proposes an improvement over the widely used sequentially linear solution procedure often utilized for fracture simulations. In the classical secant version of this method, a partial solution of a step is scaled to reach a stress limit in exactly one element and the mechanical properties of the critical element are reduced. Non-proportional loading is generally unfeasible due to avalanches of ruptures caused by stress redistribution. Because only one loading vector can be scaled at a time, all others have to remain constant during the step. However, the constant load vectors do not allow proper determination of the critical element. A modified procedure based on redistribution of released stresses is developed here. It preserves the linearity of each step. After rupture of the critical element, a sequentially linear redistribution process of stress release takes place until a static equilibrium state is reached. During the redistribution, other elements may break.

The proposed enhanced sequential procedure is also compared with another recently published "event-by-event" linear method for non-proportional loading. It is shown here, with the help of simple examples, that the proposed redistribution method yields correct results for non-proportional loading, unlike the other methods under comparison.

1. Introduction

Both lattice and continuum material representations are often used for the modeling of processes of crack propagation. Since the lattice approach is used here to demonstrate the proposed procedure, let us first mention some of the most important work done in this field.

The lattice representation was originally used for fracture in solids by physicists [1,2]. Several researchers have improved their models to render them suitable for simulating experimental data. Regarding concrete, a lot of progress was made by the Delft group in the Netherlands. They proposed the projection of a material meso-structure on top of a lattice and the assignment of lattice elements with different properties according to their position in the meso-structure [3]. Their early influential work is comprehensively summarized by Schlangen [4], including a successful comparison with many experiments. Van Vliet's dissertation [5] also presents an extensive comparison of a lattice model with experiments. The current trends include three-dimensional lattices with more realistically-shaped particles [6]. Other articles related to lattice modeling that the present authors consider to be very important are the development of a rigid-body-spring network by Bolander and Saito [7] and the work of van Mier et al. [8] studying the influence of various grain contents and properties.

Most of the lattice models use brittle elements (or piece-wise brittle elements such as can be found in [9]) in connection with the classical version of the sequentially linear solution procedure (referred to as the *secant* procedure from here on).

Continuum models can adopt the concept of a *secant* solution or any "event-by-event" strategy as well (see [10]). The procedure enables the solving of physically nonlinear tasks by a sequence of linear steps. Relations between stresses and

* Corresponding author. Tel.: +420 549 247 116; fax: +420 541 240 994.
E-mail addresses: elias.j@fce.vutbr.cz (J. Eliáš), frantik.p@fce.vutbr.cz (P. Frantík), vorechovsky.m@fce.vutbr.cz (M. Vořechovský).

0013-7944/$ - see front matter © 2010 Elsevier Ltd. All rights reserved.
doi:10.1016/j.engfracmech.2010.05.018

Nomenclature

$\|\boldsymbol{X}\|$	Euclidean norm of vector $\boldsymbol{X}$
α, β, γ, θ	characters used to distinguish between the different examples given
ΔX	reference (incremental) value of variable X
δ	prescribed displacement
λ	multiplier that scales reference elastic solutions
$\boldsymbol{\sigma}$	stresses in an element
A	cross-sectional area of element
$\boldsymbol{A}$, $\boldsymbol{B}$, $\boldsymbol{L}$	loading vectors
A, B, C, D	branches of the developed algorithm
$\boldsymbol{S}$	disequilibrium forces – external forces that acted on the removed element
$\boldsymbol{d}$	nodal displacement
E	elastic modulus
$f(\cdot)$	failure surface: $f(\cdot) = 1$ indicates failure
f_t	tensile strength
$\boldsymbol{K}$	stiffness matrix of structure
k	pointer to critical element
l	length of element
n_u	number of loading vectors
n_e	number of elements in the structure
$\boldsymbol{R}$	reactions
u	superscript denoting current loading vector
s	avalanche size
t	variable showing how much of the current loading vector has been imposed

strains have to be defined as a collection of elasto-brittle teeth, called a "saw-tooth" law. A method for constructing such a law can be found in [11]. The simplest example of such a law is elasto-brittle behavior.

Pure elasto-brittle ruptures are often assumed especially in lattice modeling; the softening observed at a structural scale is then understood as a structural effect it being a consequence of material heterogeneity (the effect of the incorporated material meso-structure) [4].

The application of standard iterative procedures to problems with jumps in constitutive law can be difficult because the energy, released in one incremental step, cannot be controlled by a step length. Recently, a special procedure [12] to optimally control the step size without any *a priori* knowledge regarding the failure pattern of the structure has been published. It is based on a monotonically increasing variable of the solid: the energy release, which always exhibits a positive rate when failure evolves in quasi-brittle (softening) materials. In this respect, the "event-by-event" methods (such as the ones published in the aforementioned papers [10,11]) also have the potential to trace the failure process in a controlled fashion. The convenience of the sequentially linear strategy for this class of problems is proved by many published texts (for instance in previously mentioned text [9]).

Fundamentally, the basis of the "event-by-event" method lies in the scaling of the solution of an elastic linear problem to reach a certain bound of linearity defined by the rupture of the most loaded element. The external load imposed on a discretized elastic domain induces stresses in a finite number of integration points/discrete elements. A critical element, k, breaks if its stress exceeds the failure criterion $f(\boldsymbol{\sigma}_k) = 1$. In each step, the solid is subjected to a reference load, $\Delta\boldsymbol{L}$, and the corresponding reference stresses $\Delta\boldsymbol{\sigma}$ are evaluated. It is assumed that, in every step, the scaling coefficient λ and element k can be uniquely determined by the following condition:

$$f(\lambda\Delta\boldsymbol{\sigma}_k) = 1 \ \wedge \ \forall h \neq k : f(\lambda\Delta\boldsymbol{\sigma}_h) < 1, \tag{1}$$

i.e. the critical element k reaches its fracture criteria when load $\lambda\Delta\boldsymbol{L}$ is imposed while all the other elements are below their strengths. The mechanical properties of the critical element k are consequently modified by jump damage. The next step starts again from the beginning (zero stresses and strains) but the stiffness of the structure is modified. The procedure is applicable to a variety of problems, even those involving snap back, and there are no complications with convergence.

The purpose of this paper is to improve the *secant* solution scheme. As will be shown later, the application of the *secant* procedure fails in cases of non-proportional loading. It is proposed that the problem be solved by the immediate *redistribution* of stresses released from ruptured elements into their neighborhood. The proposed method (denoted here as the *redistribution* method) preserves the "event-by-event" linear concept; no iterations are utilized. A complicated non-proportional load-path has to be idealized by a collection of piece-wise proportional loading vectors $\boldsymbol{L}_1, \boldsymbol{L}_2, \ldots, \boldsymbol{L}_{n_u}$ as illustrated in Fig. 1 b.

The paper begins by describing a situation where the *secant* sequentially linear solution procedure cannot be applied. It is demonstrated in Sections 2 and 3 that this concept fails when applied to non-proportional loading. In Section 4, we show how the concept of linear steps can be modified for non-proportional loading. Note that this modification can also be used

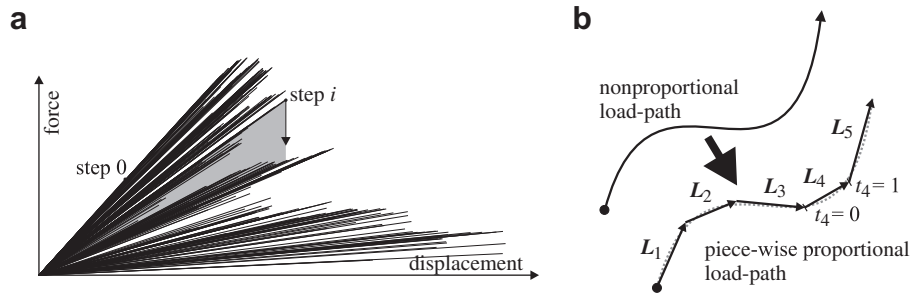

Fig. 1. (a) Example of a response of a uniaxial tensile test obtained by the *secant* sequentially linear model. The hatched area shows one avalanche of size 45 events. Keeping the displacement nondecreasing, the system would evolve through static disequilibrium states in the direction marked by the arrow. (b) Idealization of a complicated non-proportional load-path by a collection of piece-wise proportional loading vectors $\boldsymbol{L}_1, \boldsymbol{L}_2, \ldots, \boldsymbol{L}_{n_u}$.

for proportional loading. An advantage of the improved *redistribution* method over the *secant* approach is clearly shown with the help of two examples (one involving a simple lattice with just nine elements and the other involving a complex lattice model) in Section 5. Another improvement of the *secant* approach recently published in [13] (from here on called *DeJong's* method) is compared with the proposed *redistribution* method in Section 6. In the same section, we exemplify some weak points of *DeJong's* strategy by using simple examples. A detailed numerical solution of an extremely simple structure involving three springs is performed in Appendix A.

2. Avalanches of events

Physical experiments as well as numerical simulations are often conducted under displacement control because it enables the damage propagation to be kept stable. Even though there is no difference between the displacement and force control in the *secant* sequentially linear scheme, one should distinguish between those two cases during a smoothing algorithm. A series of imposed displacements or forces does not ascend all the time. Local descending parts can be understood as small instabilities and disregarded – smoothed out [14]. The smoothing can be done for the displacement axis (or force axis) in the case of displacement control (or force control respectively). These snap-backs can also be imagined as avalanches of ruptures, driven by redistribution of the elastic energy released from broken elements into their neighborhoods.

A theoretical description of such avalanches is published in the literature, for instance [15] for the case of bundles of many parallel fibers. Fiber bundle models represent a useful idealization providing a qualitative description of the avalanche phenomenology and their statistics. In fiber bundle models, an avalanche is usually defined as follows: when a structural element breaks, the increased load (force) $\boldsymbol{L}$ on the remaining elements may cause further ruptures, and thus induces a burst avalanche of a certain size s (this size is a number of elements that fail, too) is induced. The external load $\boldsymbol{L}$ performs a biased random walk and the avalanche size distribution is equivalent to the first return time distribution of the walk. Thus, avalanche size is defined as the number of springs (bonds) that break simultaneously for a constant load.

With this definition of an avalanche, Hemmer and Hansen [16] have shown that, for global load sharing in fiber bundles with random fiber thresholds, the integrated number of burst events of size s per fiber, $N(s)/N$, asymptotically follows a power law function of the form $N(s)/N \propto s^{-5/2}$ in the limit $N \to \infty$. The exponent $-5/2$ is universal in the sense that it does not depend on the statistical distribution of the individual fiber strengths. For local load sharing rules the distribution falls off with increasing burst size much faster than for global load sharing, and does not follow a power law. In lattice model simulations one can define the avalanche size s similarly: by counting the number of broken bonds that fail without any further increase in the applied load. The situation then becomes more complicated and there is no analytical solution available. Large-scale simulations with random fuse models in 2D and 3D show that the exponents depend on the lattice topology while random spring models have exponents close to $-5/2$ (see e.g. [17,18]). A detailed review on this topic can be found in [19].

One can also define the avalanche size as the number of consecutive ruptures needed to increase displacement. Fig. 1 shows an example of such an avalanche, beginning at step i, in response to a uniaxial tensile test simulation controlled by displacement increments. We have performed numerical analyses with lattice models where the uniaxial element strength is not continuously random, but give by its correspondence to aggregate, matrix and the interfacial transitional zone. Our numerical results suggest that the avalanche size has an exponential distribution as well. This phenomenon is known as an effect of self-organized criticality [20], i.e. an avalanche of any size can be expected, and there is no typical avalanche size. Assuming the exponential avalanche size distribution for our case, avalanches can occur at any time and with an arbitrary size as well.

Handling these avalanches in numerical procedures seems to be the crucial point. Each time some elasto-brittle element reaches its instantaneous strength, a certain amount of released energy has to be redistributed immediately. This redistribution is generally a *dynamic phenomenon* which passes through static disequilibrium states. The static method is obviously not able to describe the redistribution properly. Yet, we are trying to develop a quasistatic technique to handle these avalanches in order to simulate the proportional and mainly non-proportional loading of lattices.

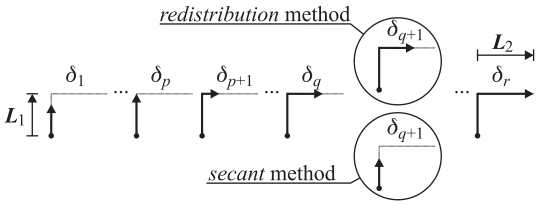

Fig. 2. Example of non-proportional loading solved by the *secant* and *redistribution* sequentially linear strategies.

3. Non-proportional loading

The sequentially linear solution is often applied in spite of the dynamic nature of the redistribution process for elasto-brittle constitutive laws. In most of these simulations, the load is considered to be proportional, i.e. the reference loading vector $\Delta\boldsymbol{L}$ is the same at any moment in the simulation (for instance the modeling of eccentric tension in [5]). However, one can find publications where the authors use the sequentially linear procedure for non-proportional loading; e.g. article [21] presents an irregular lattice of brittle beams subjected to load-paths 4a, 4b, and 4c of Nooru-Mohamed tests [22]. It will now be shown, how the *secant* procedure might give inappropriate results in such a case.

Since there is no common formulation of the *secant* strategy for non-proportional loading, we assume a straightforward application/extension of the existing concept. Fig. 2 schematically shows non-proportional loading that consists of a tensile and subsequent shear load (prescribed upward displacement followed by a movement to the right). In other words, there are two loading vectors, $\boldsymbol{L}_1(\uparrow)$ followed by $\boldsymbol{L}_2(\rightarrow)$. Solving this task by the *secant* sequentially linear concept, one reaches the end of tension (proportional part) in step p. The subsequent steps start again from the beginning, follow the tensile branch, and scale the shear vector. The avalanche starting at step q might cause an element to be unable to sustain even the first tensile loading vector and thus break before the end of the prescribed tension – step $q+1$. A criticism of this *secant* technique arises from the invalid stress field in step $q+1$. The jump back to the previous loading vector can cause the failure of an inappropriate element, because the whole instantaneous load is not imposed.

As described above in Section 2, the occurrence of a sufficiently strong avalanche that pushes the solution back to the previous loading vector is unpredictable. Thus, one should expect it at any stage of the simulation of any kind of non-proportional loading.

4. Method of gradual static stress redistribution

An enhancement of the *secant* sequentially linear method for non-proportional loading is proposed here. Each time a bar (bond) is broken, it is necessary to re-equilibrate the lattice system. Once a bar is broken, it is replaced by corresponding forces. These forces are then gradually redistributed. Once the system reaches an equilibrated state (even after an avalanche of breakages) the loading proceeds to the subsequent load increase.

Each step consists in linear scaling of the reference load, but it does not start from the beginning as in the *secant* method. The scaling factor is applied only to incremental values of variables, i.e. the concept established by Eq. (1) is transformed into the following incremental formulation:

$$f(\boldsymbol{\sigma}+\lambda\Delta\boldsymbol{\sigma})=1 \ \wedge \ \forall h\neq k : f(\boldsymbol{\sigma}+\lambda\Delta\boldsymbol{\sigma})<1, \tag{2}$$

where $\boldsymbol{\sigma}$ stands for the previously reached stress in the structure and $\Delta\boldsymbol{\sigma}$ is the stress increment caused by the newly applied load increment. The series of imposed loads (either displacements or forces) is forced to be non-decreasing, so that a proper stress field is evaluated.

The rest of this section describes one step of the algorithm. It is assumed that the load consists of a series of vectors $\boldsymbol{L}_u$, $u=1,2,\ldots,n_u$, no matter if these are forces or displacements. For instance, the first vector $\boldsymbol{L}_1$ moves one point of the structure in upwards direction to a displacement of 1 mm, and the subsequent vector $\boldsymbol{L}_2$ applies a force of 10 kN at another point in the horizontal direction. The results from the previous steps are stored in vectors of nodal displacements $\boldsymbol{d}$, reactions $\boldsymbol{R}$ and element stresses $\boldsymbol{\sigma}$. The stiffness matrix is denoted $\boldsymbol{K}$. Let us assume that the structure has already passed loading vectors $\boldsymbol{L}_1,\boldsymbol{L}_2,\ldots,\boldsymbol{L}_{u-1}$. Therefore, the current loading vector is $\boldsymbol{L}_u$ and the reference load increment constructed from it is denoted $\Delta\boldsymbol{L}_u$. We use the reference load $\Delta\boldsymbol{L}_u$ instead of $\boldsymbol{L}_u$ to deliver a more transparent description. Usually, one uses the reference load of unit size – the reference loading vector is obtained by dividing the full one by its size: $\Delta\boldsymbol{L}_u=\boldsymbol{L}_u/\|\boldsymbol{L}_u\|$. Let us define a variable $t_u\in\langle 0;1\rangle$ which says how far the structure proceeded in the loading by the current loading vector $\boldsymbol{L}_u$. It is a fraction of the total prescribed load, see Fig. 1b. When $t_u=0$, the computation with that load starts. When $t_u=1$, the process reached the end of the prescribed load $\boldsymbol{L}_u$. Each time when the procedure applies a load increment, variable t_u is increased by the size of the imposed load increment divided by the size of the current loading vector: $\Delta t_u=\lambda\|\Delta\boldsymbol{L}_u\|/\|\boldsymbol{L}_u\|$.

The proposed redistribution algorithm is divided into four branches: A, B, C and D. Every step starts at branch A; the reader can follow the items on the attached flowchart (Fig. 3).

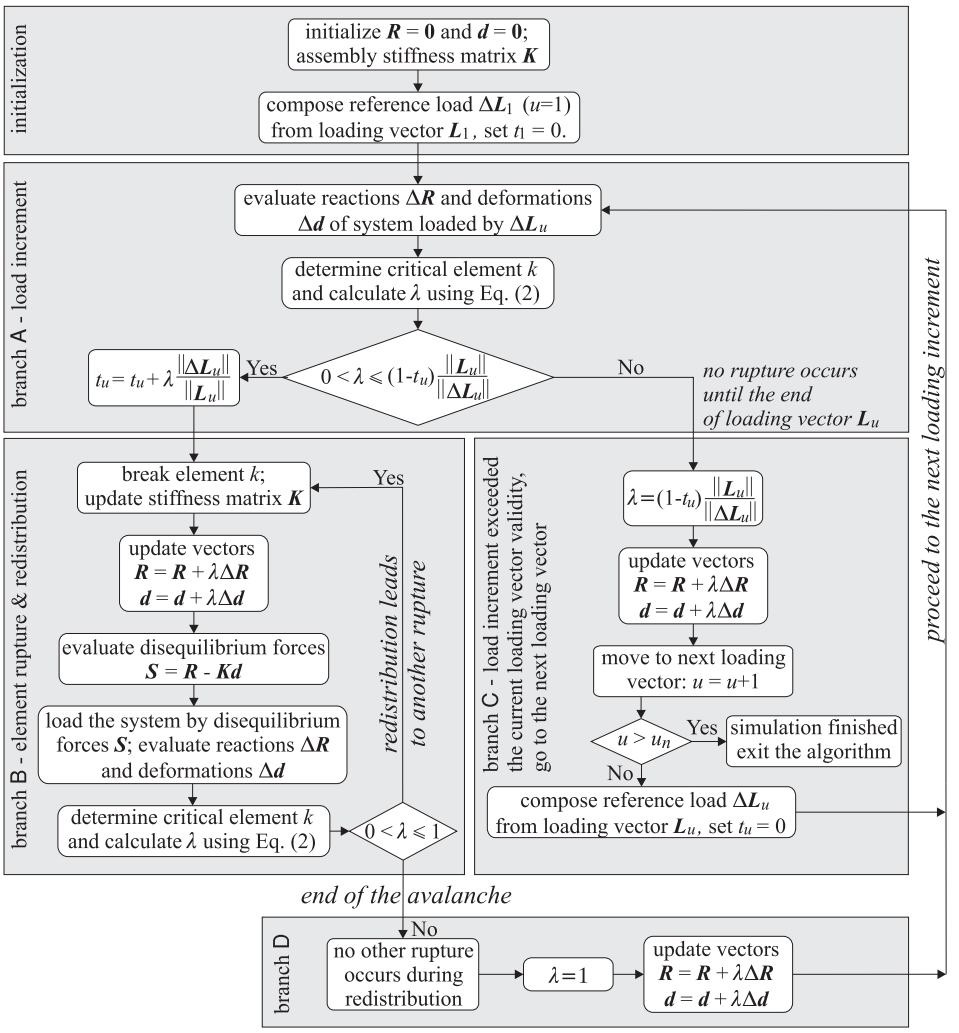

Fig. 3. Flowchart of the developed *redistribution* algorithm.

Branch A loads the structure by the prescribed load increment.

A1 Solve a linear analysis $(\Delta\boldsymbol{R},\Delta\boldsymbol{d})$ of the system loaded by $\Delta\boldsymbol{L}_u$. Evaluate the reference stress $\Delta\sigma_h$ for all elements $h \in 1,2,\ldots,n_e$.

A2 Find the critical element k and the positive multiplier λ so that the failure criterion from Eq. (2) is satisfied.

A3 Check whether the proposed load increment $\lambda\Delta\boldsymbol{L}_u$ overshoots the intended load $\boldsymbol{L}_u$. It can happen, for instance, that the vector $\boldsymbol{L}_u$ prescribes a total displacement of 1 mm but the application of the proposed $\lambda\Delta\boldsymbol{L}_u$ to break another element would move it further than 1 mm. The bound on λ is maintained by variable t_u, which cannot exceed one. Two scenarios are possible now:

(i) If the limit of the reference loading vector is exceeded

$$\lambda > (1-t_u)\frac{\|\boldsymbol{L}_u\|}{\|\Delta\boldsymbol{L}_u\|} \tag{3}$$

or $\lambda < 0$, no other rupture occurs during application of the remaining part (of size $(1-t_u)\|\boldsymbol{L}_u\|$) of vector $\boldsymbol{L}_u$. Proceed to branch C.

(ii) Otherwise, the proposed load increment is accepted and a local rupture(s) is going to occur. Save the current position in the loading:

$$t_u = t_u + \lambda\frac{\|\Delta\boldsymbol{L}_u\|}{\|\boldsymbol{L}_u\|}. \tag{4}$$

Proceed to branch B.

Branch B *redistributes* the energy from broken springs. It neither *increases* the imposed load nor *decreases* it.

B1 Element k breaks. Reduce the stiffness and strength of element k according to its constitutive law and update stiffness matrix $\boldsymbol{K}$.

B2 Update the total displacements, reactions and stresses:

$$\boldsymbol{R} = \boldsymbol{R} + \lambda\Delta\boldsymbol{R}, \tag{5}$$

$$\boldsymbol{d} = \boldsymbol{d} + \lambda\Delta\boldsymbol{d}, \tag{6}$$

$$\boldsymbol{\sigma} = \boldsymbol{\sigma} + \lambda\Delta\boldsymbol{\sigma}. \tag{7}$$

B3 The system is not in an equilibrium state because the stiffness of element k has been changed. Therefore, calculate the disequilibrium forces

$$\boldsymbol{S} = \boldsymbol{R} - \boldsymbol{K}\boldsymbol{d}. \tag{8}$$

B4 Load the structure by disequilibrium forces $\boldsymbol{S}$. This serves to relax the structure, redistributing stresses from the damaged element k into its surviving neighborhood. The results of this linear analysis are again the reactions $\Delta\boldsymbol{R}$, deformations $\Delta\boldsymbol{d}$ and elemental stresses $\Delta\boldsymbol{\sigma}$.

B5 Some other elements may break during this redistribution. The same concept is used to identify them. According to the criterion from Eq. (2), the multiplier λ and critical element k are found again.

B6 Now, the algorithm detects whether other ruptures occur:

(i) If $\lambda > 1$ or $\lambda < 0$, all the released stress can be redistributed without any other rupture. Go to branch D.

(ii) Otherwise, subsequent ruptures occur. The algorithm handles them in the same way as the previous ruptures: simply go to the beginning of branch B. This is repeated until the end of the current avalanche, i.e. until equilibrium is reached – item B6(i).

Branch C is entered after the process has reached the end of the current loading vector $\boldsymbol{L}_u$.

C1 Determine λ so that the structure is loaded by the remaining part of $\boldsymbol{L}_u$:

$$\lambda = (1 - t_u)\frac{\|\boldsymbol{L}_u\|}{\|\Delta\boldsymbol{L}_u\|}. \tag{9}$$

C2 Update the total displacements, reactions and stresses according to Eqs. (5)–(7).

C3 Now, the algorithm proceeds to the next loading vector: $u = u + 1$. Two situations are possible:

(i) There is no other loading vector ($u > u_n$) and the simulation is finished.

(ii) Otherwise, the new reference loading vector $\Delta\boldsymbol{L}_u$ has to be composed from the new load $\boldsymbol{L}_u$. Moreover, since the algorithm starts with a new load, the current parameter t_u has to be set to zero. Start again with branch A (increase the imposed load).

Branch D is entered when the redistribution is finished, i.e. the avalanche of ruptures is finished and the structure reaches the equilibrium state.

D1 To release all the disequilibrium forces, set $\lambda = 1$. We already know that this does not cause any rupture.

D2 Update the total displacements, reactions and stresses: Eqs. (5)–(7).

D3 Start again with branch A (increase the imposed load).

The algorithm is similar to the *secant* procedure in the way it finds the linear multiplier λ that leads to the rupture of exactly one element. The element is removed/damaged. However, the stress which was stored in the damaged part is released gradually. In other words, one can imagine the influence of the damaged part as disequilibrium forces that are redistributed by another sequentially linear loop(s).

The procedure can be understood as a limit state of a dynamic solution with damping approaching infinity. Such damping completely eliminates the inertial forces.

Notice that scaling parameter λ was always non-negative. A negative value of λ inside branch A would mean that we are applying load in the opposite direction. Similarly, a negative λ inside branch B would mean that, instead of damaging the critical element and redistributing the released forces, we are increasing its stiffness and unloading its neighborhood.

5. Comparison with the *secant* sequentially linear method

Let us present two examples which indicate the difference between results obtained with the *secant* approach and those obtained with the proposed *redistribution* approach.

5.1. Example with a simple lattice structure

The first numerical example involves a simple truss structure with nine bars (springs). The studied truss structure (Fig. 4) is loaded by prescribed displacements $\boldsymbol{L}_1$ and $\boldsymbol{L}_2$, firstly in the $y(\uparrow)$ and then in the $x(\rightarrow)$ direction. The aim is to find the failure

pattern after performing the prescribed motions of the top rigid platen: 1 mm up and 2 mm to the right. The loading vectors are defined in displacements: $\boldsymbol{L}_1 = (\delta_x, \delta_y)^T = (0, 0.001)^T$, $\boldsymbol{L}_2 = (0.002, 0)^T$. The bottom rigid platen is fixed. All elements are elasto-brittle springs with cross-sectional areas of 1 m^2; elements 1–4 (or 5–9) have elastic moduli of 10 GPa (or 1 GPa respectively). The tensile strengths of elements 1, 2 and 3 are 2 MPa, 1 MPa and 1.25 MPa. The remaining elements have infinite strengths.

Both the *secant* approach and the *redistribution* strategy initially proceed identically. The structure is loaded by the reference prescribed displacements $\Delta\boldsymbol{L}_1 = (0, 1)^T$. No element reaches its strength until $\lambda\Delta\boldsymbol{L}_1$ reaches the load validity limit $\lambda = \|\boldsymbol{L}_1\|/\|\Delta\boldsymbol{L}_1\|$, i.e. $\lambda = 0.001$ and $t_1 = 1$. Both procedures continue with the second reference loading vector $\Delta\boldsymbol{L}_2 = (1, 0)^T$. The overall imposed load then equals $\boldsymbol{L}_1 + \lambda\Delta\boldsymbol{L}_2$. The scaling parameter λ that leads to the first rupture was found to be 0.00185, $t_2 = 0.925$ (Fig. 4, state *D*) and the critical element has the number 1. From here on, the two approaches *differ*.

In the *secant* strategy, bar 1 is removed from the structure at this stage. The next step starts again from the beginning with the reference loading vector $\Delta\boldsymbol{L}_2 = (1, 0)^T$. Now, bar 2 breaks at $\lambda = 0.00083$ (Fig. 4, state *E*). The last step of the *secant* procedure evaluates the linear analysis for the whole load $\boldsymbol{\delta} = (0.002, 0.001)^T$ without any other rupture (Fig. 4, state *F*).

In contrast, the *redistribution* strategy does not remove bar 1 immediately. In order to maintain equilibrium, element 1 is replaced by force $F_1^A = 2.0$ kN (Fig. 4, state *A*). The force is then gradually decreased (the structure is loaded by the disequilibrium forces of state *A*). Note that this redistribution corresponds to a gradual reduction in the stiffness of element 1. When force F_1 reaches the value of 0.6 kN (or the stiffness of that element decreases to approximately 0.9 GPa), element 3 breaks. The next step then tries to diminish both the residual force of element 1 $\left(F_1^B = 0.6 \text{ kN}\right)$ and the force transmitted by element 3 $\left(F_3^B = 1.25 \text{ kN}\right)$. Because it succeeds without any other rupture, the avalanche stops and the structure attains equilibrium. Similarly as with the *secant* strategy, the reminder of the load can be imposed without any other rupture.

Note the difference: in the *secant* strategy, bar 2 was broken under pure tensile load $(0, 0.00083)^T$ in spite of the fact that the structure had previously reached the tensile–shear load combination $(0.00185, 0.001)^T$. This is unexpected, because "hard loading" does not release the whole current external load due to some local ruptures.

The obvious difference between the two final states *C* and *F* leads to a question: which solution is better? The above-mentioned dynamic character of the problem does not allow this to be judged, but the *redistribution* procedure did not violate any requirements (it always conformed with the instantaneous stress field).

5.2. Example with a large lattice structure

The example given above as well as the other examples that follow clearly demonstrate differences in the behavior of different numerical methods in the case of simple structures with very low number of elements. One might doubt whether the improvement gained from the proposed *redistribution* method has a significant effect in the case of complex lattices consisting of many elements. To demonstrate that differences also occur in simulations with several thousands of elements, we present comparisons of simulations with the structure sketched in Fig. 5a. This example is based on the prestressed structure presented in [13]. The beam is initially prestressed by a tendon (the effect of the tendon is simplified into load ***A*** of magnitude 12 kN) and then gradually loaded in bending by force ***B***. The domain is filled with rigid cells interconnected by springs, this being what is known as a rigid-body-spring network [23]. The cell geometry is provided by a Voronoi tessellation. In fact, the model is very similar to Bolander's random lattice [7]. For simplicity, we ignore the contribution of shear forces and bending moments at element facets to the failure criterion, i.e. any element breaks only when the normal stress exceeds the limit chosen here as 1 MPa. Both the beam depth and the thickness equal 0.2 m; the span is set to 0.8 m. To suppress the spurious local effect of point loading ***A***, we permitted spring breaks only in the central part of the beam – see Fig. 5a.

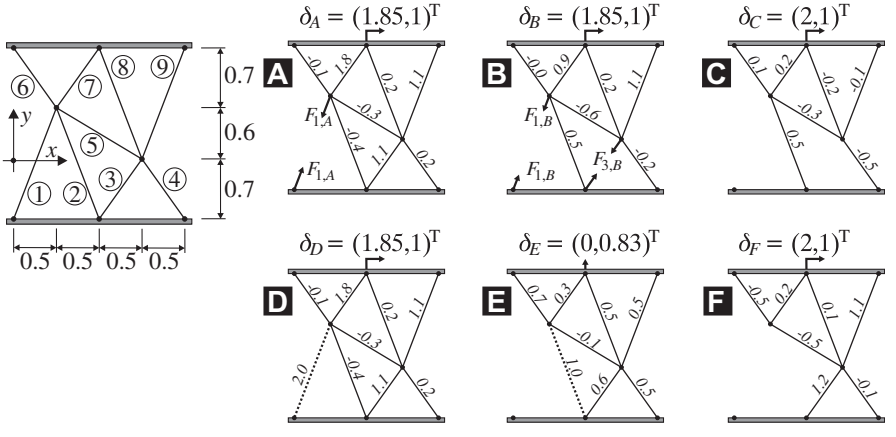

Fig. 4. Numerical example of the *redistribution* procedure (states *A*–*C*) in comparison with the *secant* sequentially linear procedure (states *D*–*F*). Prescribed displacements $\boldsymbol{\delta}$ are in millimeters and the corresponding stresses, written above the elements, are in megapascals.

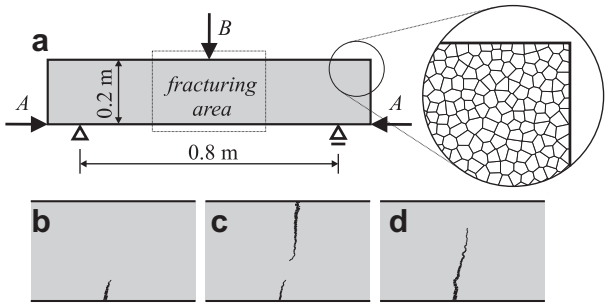

Fig. 5. Comparison of the *secant* and *redistribution* methods. (a) Prestressed structure considered for comparison. (b and c) Crack pattern in the early and final stages of the solution provided by the *secant* method. (d) Final crack obtained by the proposed *redistribution* method.

The initial load ***A*** leads to tension in the upper layer of the beam; however, the stress limit is not exceeded in any spring. Then, force ***B*** starts to reduce tension in the upper half and gradually induces tension in the bottom layer. Finally, a fracture initiates from the bottom surface. In the *redistribution method*, load ***B*** is not removed and the compression of the upper layer remains. The fracture therefore continues to propagate further from the bottom, see Fig. 5d.

The *secant* method removes the whole of the applied load after every rupture and starts again with pure load ***A*** (if possible followed by the second loading vector ***B***). Thus, tension in the upper layer due to load ***A*** is recovered at the beginning of every step. The crack propagating from the bottom due to load ***B*** weakens the beam's cross section. Once the crack reaches a certain size (Fig. 5b) it causes the beam to become unable to sustain the whole initial prestressing load ***A*** and the beam starts to fracture from the top (Fig. 5c) under pure load ***A*** alone. This result apparently does not correspond to the expected and experimentally observed behavior of such a beam.

Note that for this illustrative example we have selected a structure which is inconvenient for the *secant* method. In many other real loading situations, both methods would probably yield very similar crack patterns. This is also the case of matching the experimental crack patterns of non-proportional Nooru-Mohamed tests using the *secant* method [21,4].

6. Comparison with *DeJong's* sequentially linear method

The objection against the *secant* approach described in Section 3 and demonstrated by Section 5 is supposed to be avoided by a recently published enhancement [13], here called *DeJong's* method. However, according to the present authors, discrepancies remain, though less obvious; we will show that *DeJong's* procedure also does not handle ruptures correctly (i.e. we claim that ruptures can occur under an invalid stress field).

In order to demonstrate the weak point of *DeJong's* method, we present two numerical examples. Before doing so, an imaginary task without any direct structure representation is used to reveal the difference between the two methods under comparison. Then, the rupture of two truss structures is examined briefly by both procedures.

Article [13] (*DeJong's* method) proposed the solution of non-proportional loading by modification of the scaling method. In agreement with article [13], let us consider two load cases $\boldsymbol{A} = \boldsymbol{L}_1$ and $\boldsymbol{B} = \boldsymbol{L}_2$. Assume that the simulation has already proceeded into load case ***B*** (the whole load ***A*** has already been applied). By scaling the load vector ***B***, *DeJong's* method simply tries to find a state in which all the elements except the critical one are below their failure criteria (strengths). Scaling factor λ_h, which leads to rupture, is found for every element h. The set of elements is divided into two parts: those where an increasing load ***B*** *increases* the elements' stresses, and those where the same load *decreases* their stresses. The minimum factor $\lambda^t_{\min}$ is found in the former part, whereas the maximum factor $\lambda^c_{\max}$ is selected from the latter part. When $\lambda^c_{\max} < \lambda^t_{\min}$, the required state exists and the element with scaling factor $\lambda^t_{\min}$ breaks. In the opposite case ($\lambda^c_{\max} > \lambda^t_{\min}$), such a solution cannot exist because there is always at least one element that violates the failure criteria (stress is above its strength). However, the algorithm proceeds via the rupture of the element with the scaling factor $\lambda^c_{\max}$.

DeJong's method does not take into account the previously achieved amount of load vector ***B***. In contrast, the proposed method of gradual static stress *redistribution* does reflect all previously applied loads. A schematic comparison is provided in Fig. 6. The imaginary structure consists of three bars 1–3. There are two alternative forms of the structure studied, α and β, and the difference is in the response of bar 3. In both structures α and β, bar 3 breaks in the first step, and therefore in the next step there will be only two bars. The only remaining difference between them will be the load level at which bar 3 breaks, i.e. the previously applied load. The vertical axis shows the stresses in the bars, whereas the horizontal axis represents the load (i.e. evolution of the load through scaling factor λ). In the first step (Fig. 6a), the structure passes the loading vector ***A***. By scaling the load ***B*** in the second step, bar 3 reaches its strength and breaks. In the first structure, bar 3 breaks at state α_2, whereas in the second one, rupture occurs at state β_2.

In the third step depicted in Fig. 6b, the factors $\lambda^t_{\min}$ and $\lambda^c_{\max}$ are found according to *DeJong's* procedure. As apparent from Fig. 6b, an increase in load ***B*** leads to an increase in the stress of bar 1 and simultaneously to a stress decrease in bar 2. Since only these two bars remain, $\lambda^t_{\min}$ is dictated by bar 1 and $\lambda^c_{\max}$ by bar 2. Because $\lambda^c_{\max} < \lambda^t_{\min}$, the scaling factor $\lambda^t_{\min}$ is selected

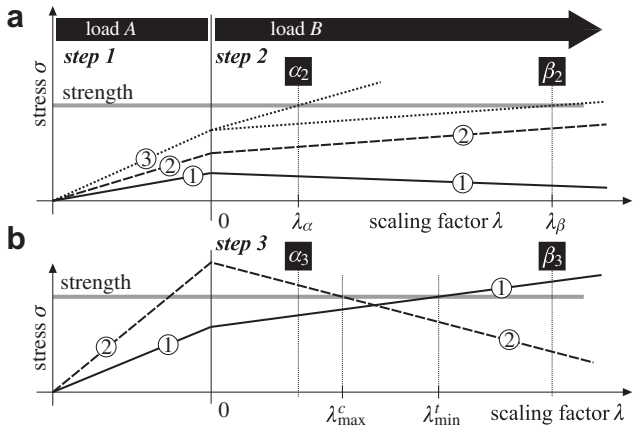

Fig. 6. Evolution of stresses in the structure during non-proportional loading. (a) Stresses in the three bars after the application of loads ***A*** and ***B***. (Common to all three linear methods.) (b) Stresses in the two remaining bars after the removal of bar 3 (in both structures α and β the stresses are identical). The left part corresponds to an increasing load ***A***, the right part corresponds to an increasing load ***B***.

and bar 1 breaks. This happens in both distinguished cases α and β – irrespective of the rupture of bar 3 (the difference between the two structures α and β is ignored). Note that in Fig. 6b, the load levels that led to the rupture of beam 3 (i.e. previously reached load levels) are marked by symbols α_3 and β_3.

In contrast with the third step of *DeJong's* procedure, the *redistribution* method loads the structure with disequilibrium forces and pushes it by redistribution from state α_2 [or β_2] into state α_3 [or β_3 respectively] – Fig. 7a and b. During this redistribution, different bars break in each of the two variants.

Again, we have a situation where the proposed *redistribution* method yields different results than the other method – here *DeJong's* procedure. The proposed solution respects the instantaneous load and therefore should be marked as the correct one. *DeJong's* method gave identical results in both structures, no matter how much of load ***B*** was imposed to break the first element.

In order to explain the described difference comprehensively, we provide two simple examples demonstrating the difference between *redistribution* and *DeJong's* method. This time, we also provide a mechanical model of the structure.

6.1. Two simple examples

Assume a simple structure consisting of five elasto-brittle trusses (bars) connected with two rigid platens through hinges as sketched in Fig. 8. All the bars share the same length, $l = 1$ m, the distance between all pairs of neighboring beams is 1 m, and the truss elements are numbered (no. 1 marks the top bar). Bars 1, 4, 5 have the finite tensile strength $f_t = 0.3$ kPa; bars 2 and 3 have infinite strengths.

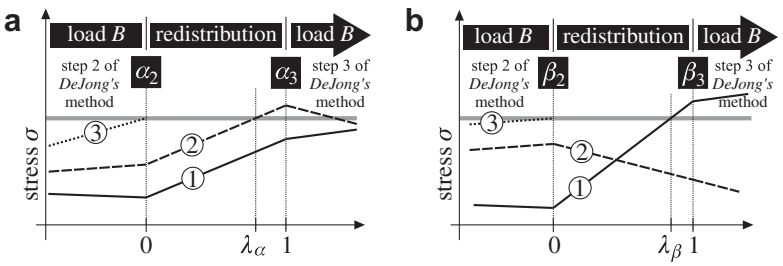

Fig. 7. Evolution of stresses during the redistribution of stress from broken beam 3.

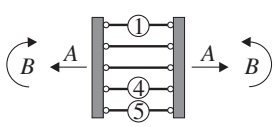

Fig. 8. Simple structure considered in order to explain the difference between *redistribution* and *DeJong's* method.

The structure is loaded by a combination of two loads, ***A*** and ***B***. Both of the loads act always in the current centroid of the bar forces. Thus, the point of action immediately moves upon rupture of any bar.

Load ***A*** represents a tensile force resulting purely in horizontal separation of the platens (no rotation of the platens is allowed meaning that the tensile force always acts in the current centroid of the bar forces). Load ***B*** represents a moment imposing pure rotation of the platens around the current centroid of the bar forces.

First, load ***A*** (force) of magnitude 1 kN is applied, then load ***B*** (moment) of magnitude 0.2 kN m.

Two different sets of elastic moduli and cross-sectional areas will be considered to demonstrate the difference between the two solution methods under comparison.

For the first case (denoted γ), the elastic moduli E and cross-sectional areas A are given in Table 1. The evolution of stresses in the system can be traced from Fig. 9a. The application of load ***A*** does not result in any rupture. Next, by applying load ***B*** in step 2 of a reference value 1 kN m, the scaling factors of bars with finite strengths are computed and presented in the same table. Using *DeJong's* approach, $\lambda^c_{\max} < \lambda^t_{\min}$ and bar 5 breaks. The same rupture occurs when using the proposed *redistribution* method because bar 5 has the smallest positive multiplier. In the third step, *DeJong's* method gives two scaling factors (Table 1), and again $\lambda^c_{\max} < \lambda^t_{\min}$, so bar no. 4 breaks. No other rupture occurs in the system until load ***B*** reaches its limit of 0.2 kN m. However, the method of gradual static stress *redistribution* introduces the redistribution of stresses from broken bar 5. Fig. 9a clearly shows that, during the transition of the structure from state γ_2 to state γ_3 by redistribution, bar no. 1 breaks. States γ_2 and γ_3 again refer to the load level that broke the first bar (the subscript denotes the step number). Both methods initially broke bar no. 5. However, the second broken bar was different. This is because the proposed *redistribution* method reflects the whole loading history while *DeJong's* method does not.

For the second case (denoted θ), the elastic moduli E and areas A are given by Table 2. Similarly as in the previous case, the stress evolution in the bars is shown in Fig. 9b. Applying the whole load ***A*** and scaling load ***B***, multipliers for bars with finite strengths are evaluated (Table 2). In the second step, $\lambda^c_{\max} < \lambda^t_{\min}$ and both *DeJong's* and the *redistribution* method remove bar

Table 1
Truss properties and scaling factors from example γ.

Truss	E (GPa)	A (m^2)	f_t (kPa)	Step 2	Step 3
1	3	1	0.3	$\lambda^c_{\max} = -0.115$	$\lambda^c_{\max} = 0.233$
2	1	1	∞	–	–
3	1	1	∞	–	–
4	1	3	0.3	$\lambda^t = 7.063$	$\lambda^t_{\min} = 1.633$
5	3	1	0.3	$\lambda^t_{\min} = 0.138$	–

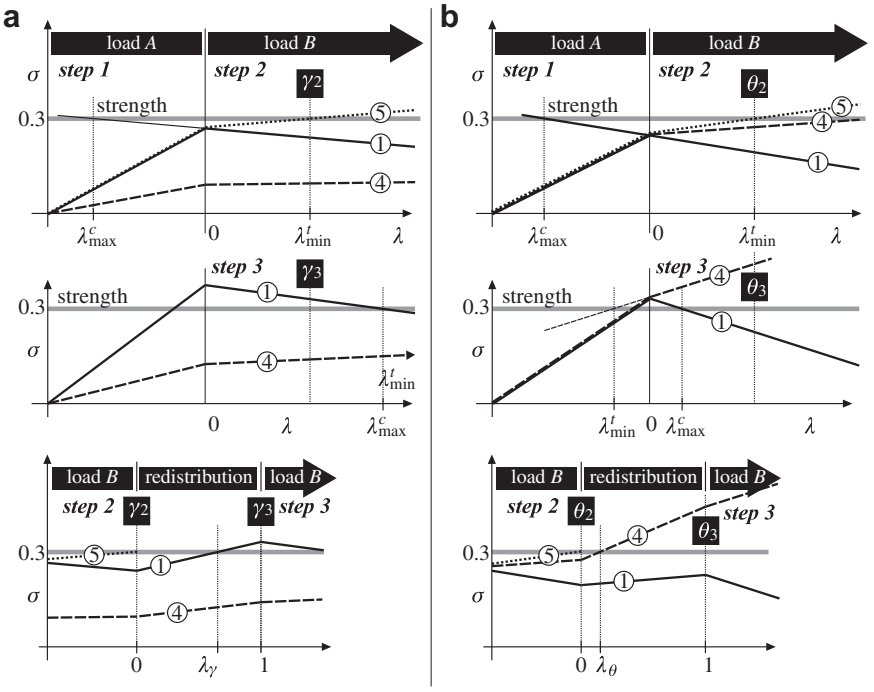

Fig. 9. Evolution of stresses in two structures (a) γ and (b) θ.

Table 2
Truss properties and scaling factors from example θ.

Truss	E (GPa)	A (m^2)	f_t (kPa)	Step 2	Step 3
1	1	0.5	0.3	$\lambda^c_{\max} = -0.175$	$\lambda^c_{\max} = 0.061$
2	1	1	∞	–	–
3	1	1	∞	–	–
4	1	0.5	0.3	$\lambda^t = 0.425$	$\lambda^t_{\min} = -0.061$
5	1	1	0.3	$\lambda^t_{\min} = 0.198$	–

no. 5. In the third step, $\lambda^c_{\max} > \lambda^t_{\min}$ and according to *DeJong's* procedure, no solution of Eq. (2) exists, but bar no. 1 is removed. In the *redistribution* method, force redistribution takes place and the internal loop of the redistribution process always has a solution. Now, bar 4 breaks during the redistribution loop, see Fig. 9b. Again, we obtained different sets of broken bars at the end of the loading processes of the two methods compared.

7. Conclusions

The applicability and possible enhancements of the sequentially linear solution method, based on the scaling of elastic steps, have been discussed. Two existing methods, namely the *secant* approach and the method proposed by *DeJong* et al. in [13], were examined and compared with the newly proposed *redistribution* procedure. It was found that the *secant* method is not *generally* applicable for non-proportional loading paths, because unloading to the origin at every local rupture does not correspond to the actual loading history. *DeJong's* approach brings about only a partial improvement. We have shown that under non-proportional loading, *DeJong's* approach leads easily to a sequence of ruptures that does not correspond to instantaneously applied load.

The proposed method of gradual static stress *redistribution* takes into account all the previously applied load. No additional computational costs are added, all the steps inside the redistribution loops are linear, they lead to element removals and no iterations are required. The procedure is applicable in both discrete and continuum MKP models (such as [10,11])

A direct comparison of the three examined techniques leads to the following conclusions:

- The *secant* strategy allows the solution process to skip back to the previous loading vectors (even to the very origin, see the solid circle in Fig. 1b). In this respect, it does not correspond to the real hard-loading situation.
- *DeJong's* procedure cannot skip to the previous loading vectors, but within the last loading vector $\boldsymbol{L}_u$ it can skip back as well.
- The described *redistribution* procedure cannot skip back (unload and reload) at all. The entirety of the previously applied load is always considered. In this way it reflects the real loading.

According to our experience, the proposed algorithm can be simply connected with the method of inelastic forces (MIF) developed by Jirásek and Bažant [24,25]. Such a combination leads to significant acceleration of the linear elastic problems solved in every step.

Unfortunately, the new *redistribution* method does not allow the observation of snap-backs; such a phenomenon is skipped in the redistribution loop by finding the static equilibrium state at the same load level, see Fig. 1. Therefore, it can be more convenient to use the *secant* procedure for proportional loading. It should be noted that the results obtained by the *secant* and *redistribution* procedure may differ even in the case of proportional loading. This is caused by the different concept of passing through the avalanches of ruptures, and there is no way to judge which of these static methods is better for solving such a dynamic phenomenon.

The *redistribution* method has been successfully used for simulating Nooru-Mohamed's experiments [22] and Petersen's experiments [26]. The published results can be found in [27,28].

Acknowledgement

This research was conducted with the financial support of the Ministry of Education, Youth and Sports of the Czech Republic under Project No. MSM0021630519. Additionally, the second and third authors acknowledge financial support of the Czech Science Foundation under Projects Nos. 103/07/1276 and P105/10/J028, respectively.

Appendix A. Detailed example of a numerical solution

In order to further illustrate the proposed enhancement, the failure of the structure plotted in Fig. 10 will now be solved by the *redistribution* procedure. It consists of three ideally elasto-brittle springs/elements with the same areas equal to 1, different Young's moduli ($E_1 = 10$, $E_2 = 2$, $E_3 = 6$) and different tensile strengths ($f_{t,1} = 5$, $f_{t,2} = 2$, $f_{t,3} = \infty$). The length of all elements is 1. Three degrees of freedom, vertical displacements of nodes 1–3, are considered and stored in vector $\boldsymbol{d}$. The structure is loaded by a prescribed deformation δ in node 3 up to displacement 2 ($\|\boldsymbol{L}_1\| = 2$). Failure occurs when the stress

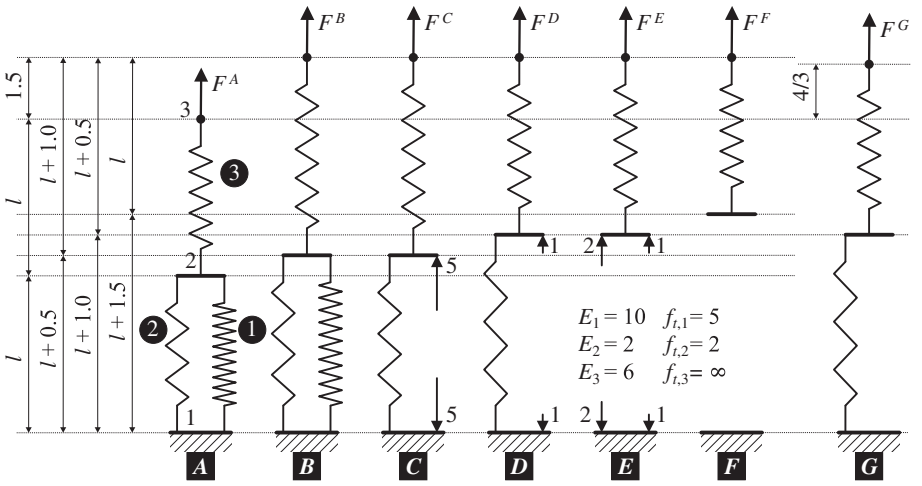

Fig. 10. Structure used in Appendix A to explain the method of gradual static stress redistribution.

in any element reaches the tensile strength of that element. Letters *A*–*G*, which mark different states of the structure in Fig. 10, are used in the following as a superscript which connects the matrices with the figure.

Initially, stresses $\boldsymbol{\sigma}$ in all springs are zero as well as the displacements of nodes $\boldsymbol{d}$ and reactions $\boldsymbol{R}$ (state *A*):

$$\boldsymbol{\sigma}^A = \boldsymbol{d}^A = \boldsymbol{R}^A = \begin{pmatrix} 0 \\ 0 \\ 0 \end{pmatrix}$$

The elastic stiffness matrix for the structure is assembled as

$$\boldsymbol{K}^A = \begin{pmatrix} E_1 + E_2 & -E_1 - E_2 & 0 \\ -E_1 - E_2 & E_1 + E_2 + E_3 & -E_3 \\ 0 & -E_3 & E_3 \end{pmatrix} = \begin{pmatrix} 12 & -12 & 0 \\ -12 & 18 & -6 \\ 0 & -6 & 6 \end{pmatrix}$$

In step 1, the reference prescribed deformation $\Delta\boldsymbol{L}_1$ is composed, t_1 is set to zero and the elastic reference step solution is calculated.

$$\Delta\boldsymbol{L}_1 = \begin{pmatrix} 0 \\ - \\ 1 \end{pmatrix} \quad \Delta\boldsymbol{d}^A = \begin{pmatrix} 0 \\ 1/3 \\ 1 \end{pmatrix} \quad \Delta\boldsymbol{R}^A = \begin{pmatrix} -4 \\ 0 \\ 4 \end{pmatrix} \quad \Delta\boldsymbol{\sigma}^A = \begin{pmatrix} 10/3 \\ 2/3 \\ 4 \end{pmatrix}$$

Obviously, when stress $\Delta\boldsymbol{\sigma}^A$ is multiplied by $\lambda = 3/2$, element number 1 reaches its tensile strength whereas all the others are below their strengths. Then, instantaneous stresses, displacements, and reactions are evaluated (state *B*), the mechanical properties of element 1 are decreased ($E_1 = 0$) and the stiffness matrix of the structure is modified. Parameter t is increased $t_1 = t_1 + \lambda\|\Delta\boldsymbol{L}_1\|/\|\boldsymbol{L}_1\| = 3/4$.

$$\boldsymbol{d}^{B,C} = \boldsymbol{d}^A + \lambda\Delta\boldsymbol{d}^A = \begin{pmatrix} 0 \\ 0.5 \\ 1.5 \end{pmatrix} \quad \boldsymbol{R}^{B,C} = \boldsymbol{R}^A + \lambda\Delta\boldsymbol{R}^A = \begin{pmatrix} -6 \\ 0 \\ 6 \end{pmatrix}$$

$$\boldsymbol{\sigma}^{B,C} = \boldsymbol{\sigma}^A + \lambda\Delta\boldsymbol{\sigma}^A = \begin{pmatrix} 5 \\ 1 \\ 6 \end{pmatrix} \quad \boldsymbol{K}^B = \boldsymbol{K}^A \neq \boldsymbol{K}^C = \begin{pmatrix} 2 & -2 & 0 \\ -2 & 8 & -6 \\ 0 & -6 & 6 \end{pmatrix}$$

Disequilibrium forces $\boldsymbol{S}^C$ then act as an additional loading vector (state *C*) and the elastic solution of the modified structure, supported in nodes 1 and 3, is calculated.

$$\boldsymbol{S}^C = \boldsymbol{R}^C - \boldsymbol{K}^C\boldsymbol{d}^C = \begin{pmatrix} -6 \\ 0 \\ 6 \end{pmatrix} - \begin{pmatrix} -1 \\ -5 \\ 6 \end{pmatrix} = \begin{pmatrix} -5 \\ 5 \\ 0 \end{pmatrix}$$

$$\Delta\boldsymbol{d}^C = \begin{pmatrix} 0 \\ 5/8 \\ 0 \end{pmatrix} \quad \Delta\boldsymbol{R}^C = \begin{pmatrix} 15/4 \\ 0 \\ -15/4 \end{pmatrix} \quad \Delta\boldsymbol{\sigma}^C = \begin{pmatrix} - \\ 5/4 \\ -15/4 \end{pmatrix}$$

This elastic solution is again scaled by factor λ and summed with the previous one to fulfill the failure criterion in exactly one element $\Rightarrow\lambda$ is equal to 4/5 and the critical element is spring number 2 (state D). The Young's modulus of element 2 is set to zero.

$$\boldsymbol{d}^{D,E} = \boldsymbol{d}^{C} + \lambda\Delta\boldsymbol{d}^{C} = \begin{pmatrix} 0 \\ 1 \\ 1.5 \end{pmatrix} \quad \boldsymbol{R}^{D,E} = \boldsymbol{R}^{C} + \lambda\Delta\boldsymbol{R}^{C} = \begin{pmatrix} -3 \\ 0 \\ 3 \end{pmatrix}$$

$$\boldsymbol{\sigma}^{D,E} = \boldsymbol{\sigma}^{C} + \lambda\Delta\boldsymbol{\sigma}^{C} = \begin{pmatrix} - \\ 2 \\ 3 \end{pmatrix} \quad \boldsymbol{K}^{D} = \boldsymbol{K}^{C} \neq \boldsymbol{K}^{E} = \begin{pmatrix} 0 & 0 & 0 \\ 0 & 6 & -6 \\ 0 & -6 & 6 \end{pmatrix}$$

Now, new disequilibrium forces are evaluated, the structure is again subjected to these forces (state E) and the elastic reference solution is performed.

$$\boldsymbol{S}^{E} = \boldsymbol{R}^{E} - \boldsymbol{K}^{E}\boldsymbol{d}^{E} = \begin{pmatrix} -3 \\ +3 \\ 0 \end{pmatrix}$$

$$\Delta\boldsymbol{d}^{E} = \begin{pmatrix} 0 \\ 1/2 \\ 0 \end{pmatrix} \quad \Delta\boldsymbol{R}^{E} = \begin{pmatrix} 3 \\ 0 \\ -3 \end{pmatrix} \quad \Delta\boldsymbol{\sigma}^{E} = \begin{pmatrix} - \\ - \\ -3 \end{pmatrix}$$

Scaling of this elastic solution does not lead to any positive λ, so λ is set to be 1 and the final avalanche vectors are evaluated (state F).

$$\boldsymbol{d}^{F} = \boldsymbol{d}^{E} + \lambda\Delta\boldsymbol{d}^{E} = \begin{pmatrix} 0 \\ 1.5 \\ 1.5 \end{pmatrix}$$

$$\boldsymbol{R}^{F} = \boldsymbol{R}^{E} + \lambda\Delta\boldsymbol{R}^{E} = \begin{pmatrix} 0 \\ 0 \\ 0 \end{pmatrix}$$

$$\boldsymbol{\sigma}^{F} = \boldsymbol{\sigma}^{E} + \lambda\Delta\boldsymbol{\sigma}^{E} = \begin{pmatrix} - \\ - \\ 0 \end{pmatrix}$$

Applying the remainder of the prescribed load $\boldsymbol{L}_1$ does not lead to any rupture, so it is skipped here.

Note that in this example, the *secant* strategy produces the same results. The *secant* algorithm starts in state A and finds the maximal load in state B. The next step begins again from zero load (but without spring number 1) and the gradual loading reaches the rupture of spring number 2 in state G. This spring is removed as well and the final state with deformation 2 of the top node is reached.

References

[1] Roux S, Guyon E. Mechanical percolation: a small beam lattice study. J Phys Lett 1985;46(21):999–1004. doi:10.1051/jphyslet:019850046021099900.

[2] Herrmann HJ, Hansen A, Roux S. Fracture of disordered, elastic lattices in two dimensions. Phys Rev B 1989;39(1):637–48. doi:10.1103/PhysRevB.39.637.

[3] Schlangen E, van Mier JGM. Simple lattice model for numerical simulation of fracture of concrete materials and structures. Mater Struct 1992;25(9):534–42. doi:10.1007/BF02472449.

[4] Schlangen E. Experimental and numerical analysis of fracture processes in concrete. PhD thesis, Delft University of Technology, Netherlands; 1993.

[5] van Vliet MRA. Size effect in tensile fracture of concrete and rock. PhD thesis, Delft University of Technology, Delft, Netherlands; 2000.

[6] Man H-K, van Mier JGM. Size effect on strength and fracture energy for numerical concrete with realistic aggregate shapes. Int J Fract 2008;154:61–72. doi:10.1007/s10704-008-9270-y.

[7] Bolander JE, Saito S. Fracture analyses using spring networks with random geometry. Eng Fract Mech 1998;61(5–6):569–91. doi:10.1016/S0013-7944(98)00069-1.

[8] van Mier JGM, van Vliet MRA, Wang TK. Fracture mechanisms in particle composites: statistical aspects in lattice type analysis. Mech Mater 2002;34(11):705–24. doi:10.1016/S0167-6636(02)00170-9.

[9] Bolander JE, Hikosaka H, He W-J. Fracture in concrete specimens of different scale. Eng Comput 1998;15(8):1094–116. doi:10.1108/02644409810244156.

[10] Rots JG, Invernizzi S. Regularized sequentially linear saw-tooth softenning model. Int J Numer Anal Methods Geomech 2004;28(7–8):821–56. doi:10.1002/nag.371.

[11] Rots JG, Belletti B, Invernizzi S. Robust modeling of RC structures with an "event-by-event" strategy. Eng Fract Mech 2008;75(3–4):590–614. doi:10.1016/j.engfracmech.2007.03.027.

[12] Gutiérrez MA. Energy release control for numerical simulations of failure in quasi-brittle solids. Commun Numer Methods Eng 2004;20(1):19–29. doi:10.1002/cnm.649.

[13] DeJong MJ, Hendriks MAN, Rots JG. Sequentially linear analysis of fracture under non-proportional loading. Eng Fract Mech 2008;75(18):5042–56. doi:10.1016/j.engfracmech.2008.07.003.

[14] van Mier JGM, Chiaia BM, Vervuurt A. Numerical simulation of chaotic and self-organizing damage in brittle disordered materials. Comput Methods Appl Mech Eng 1997;142:189–201. doi:10.1016/S0045-7825(96)01128-0.
[15] Hansen A, Hemmer PC. Burst avalanches in bundles of fibers: local versus global load-sharing. Phys Lett A 1994;184:394–6. doi:10.1016/0375-9601(94)90511-8.
[16] Hemmer PC, Hansen A. The distribution of simultaneous fiber failures in fiber bundles. J Appl Mech 1992;59(4):909–14. doi:10.1115/1.2894060.
[17] Nukala PKVV, Zapperi S, Simunovic S. Statistical properties of fracture in a random spring model. Phys Rev E 2005;71(6):066106. doi:10.1103/PhysRevE.71.066106.
[18] Zapperi S, Nukala PKVV, Simunovic S. Crack avalanches in the three-dimensional random fuse model, Physica A: Statistical Mechanics and its Applications 357 (1) (2005) 129 – 133, physics Survey of Irregular Systems - Proceedings of the International Workshop on Physics Survey of Irregular Systems, in honor of Professor Bernard Sapoval. doi:10.1016/j.physa.2005.05.071.
[19] Alava MJ, Nukala PKVV, Zapperi S. Statistical models of fracture. Adv Phys 2006;55(3–4):349–476. doi:10.1080/00018730300741518.
[20] Buchanan M. Ubiquity: why catastrophes happen. New York: Three Rivers Press; 2002.
[21] Nooru-Mohamed MB, Schlangen E, van Mier JGM. Experimental and numerical study on the behavior of concrete subjected to biaxial tension and shear. Adv Cem Based Mater 1993;1(1):22–37. doi:10.1016/1065-7355(93)90005-9.
[22] Nooru-Mohamed MB. Mixed-mode fracture of concrete: an experimental approach. PhD thesis, Delft University of Technology, Delft, Netherlands; 1992.
[23] Kawai T. New discrete models and their application to seismic response analysis of structures. Nucl Eng Des 1978;48(1):207–29 (Special Issue Structural Mechanics in Reactor Technology – Smirt-4. doi:10.1016/0029-5493(78)90217-0).
[24] Jirásek M, Bažant ZP. Macroscopic fracture characteristics of random particle systems. Int J Fract 1994;69(3):201–28. doi:10.1007/BF00034763.
[25] Jirásek M, Bažant ZP. Particle model for fracture and statistical micro–macro correlation of material constants. In: Wittmann FH, editor. Fracture mechanics of concrete structures, proceedings of FRAMCOS-2. AEDIFICATIO Publishers; 1995. p. 955–64.
[26] Petersen RB. Fracture mechanical analysis of reinforced concrete – experiments and fem modelling. Master's thesis, Department of Civil Engineering, Technical University of Denmark, Anker Engelundsvej 1, 2800 Kgs. Lyngby, Denmark; 2008.
[27] Eliáš J. Discrete simulation of fracture processes of disordered materials. PhD thesis, Brno University of Technology, Faculty of Civil Engineering, Brno, Czech Republic; 2009.
[28] Skoček J, Eliáš J, Stang H. Discrete modeling of mixed-mode crack growth in concrete. In: Cho, Meyer, Bićanić, editors. The proceedings of the first international conference on computational technologies in concrete structures (CTCS'09), Jeju, Korea; 2009. p. 258.